A Versatile Emulator for Physical Human-Robot Hand Interactions to Alter Human Walking

Mengnan Wu[1,*], Yingxin Qiu[2], Jun Ueda[2], Lena H. Ting[1,3]
[1]W. H. Coulter Department of Biomedical Engineering, Emory University and Georgia Institute of Technology, 30332-4250, Atlanta, USA
[2]George W. Woodruff School of Mechanical Engineering, Georgia Institute of Technology, 771 Ferst Drive, 30332-0405, Atlanta, USA
[3]Department of Rehabilitation Medicine, Division of Physical Therapy, Emory University, 30332-0425, Atlanta, USA
*corresponding author: mengnan.wu@emory.edu

***Abstract*—Robotic assistive and rehabilitative devices for walking based on physical interactions at the hands have promise but we do not know how best to design them to improve how people walk. Here, we validate the performance of a novel hand-contact robotic device capable of emulating a variety of physical interactions at the hands to alter human gait parameters. Slidey is a linear stage translating on a 5m track that is capable of high-fidelity current control, position control, and admittance control well within and beyond that needed to emulate human-human interactions at the hand during gait. We show proof-of-concept that novel pulsatile velocity profiles of the robotic handle can differentially alter step frequency and step length. The robotic emulator can therefore be used to identify and test controllers that could be implemented on mobile robotic walking aids in the future.**

Keywords—physical human-robot interaction, robotic emulator, robotic walking aids, hand interactions and walking

I. Introduction

Principles from physical human-human interaction (pHHI) have the potential to be applied to robotic controllers to make physical human-robot interactions (pHRI) more intuitive and seamless. However, no existing devices have been validated to have sufficient performance to emulate human-human hand interactions that affect walking. Evidence from pHHI show that human pairs intuitively alter walking behavior in response to physical hand interactions without explicit instructions, including synchronizing gait phase [1], [2], communicating walking transitions [3], and aiding balance during walking [4]. Devices designed for pHRI must be capable of emulating human hand and walking behavior to exploit principles from pHHI to aid walking.

Controllers designed to explicitly alter human walking through hand interactions have only begun to be explored in pHRI [5]–[8]. To date, instrumented passive walkers show that hand/arm forces are related to spatiotemporal gait parameters [9], [10], but such studies have not been conducted in motorized robotic walkers. Changes in a person's step width have been observed when walking with a mobile robot that follows the human's walking speed while providing light touch at the hand in the vertical direction (< 5N, verified post-hoc) [7]. Mean walking speed and step length can be increased using a constant anterior-posterior tensile force applied to a person's hand (similar to walking a dog) by a fixed-in-space robot during treadmill walking [5], [6] or a mobile robot during overground walking [8]. When a humanoid robot follows a human's stepping via forces at the hand, gait speed increases when the robot admittance gain and arm stiffness increase [11].

Because each of the previous robotic devices interacting with humans at the hand were unique in physical design and employed distinct controllers, it remains unclear whether the particular hardware design, controller, or combination of the two caused the changes observed in gait. Hand-contact robotic walking aids have either employed some type of force control [5]–[8] or admittance control with only a damping term [11]. In particular, the fixed-in-space device [5], [6] required using a self-paced treadmill with its own controller that may have also affected gait parameters.

Testing biologically-inspired human-robot controllers to alter walking via hand interactions requires sufficient bandwidth to match frequencies found in human movement. Normal human walking has a kinematic bandwidth of 4-6 Hz [12], and torques exerted at the hand for physical communication during seated human-human upper-limb interactions reach about 12hz [13]. Robot performance was not provided for the mobile robotic devices in [7], [8], and the mobile robot in [11] showed significant decrease in power at frequencies over ~3Hz.

Moreover, no existing device has demonstrated the ability to alter specific gait parameters in a systematic manner, an important function for a walking aid. During unaided human gait there is a constant relationship between step length and step frequency [14], [15], but the ability to flexibly adjust these gait parameters independently is necessary for different walking contexts (e.g. walking on stepping stones). Gait parameters are also affected in motor pathologies, e.g. individuals with Parkinson's disease take shorter steps at unimpaired step frequencies, and this motor deficit can be exacerbated by using a conventional cane or wheeled walker [16]. Although larger forces at the hand increase gait speed, these changes were also coupled to increases in step/stride length [5], [6], [8] and did not alter the step length-step frequency relationship. Further, varying the robot's admittance gain did not affect gait speed or step frequency in [11].

Our goal was to build a versatile emulator to with the capability of testing a variety of controllers with the goal of altering humans gait parameters through physical interactions at the hands. We validated the performance of a robotic handle that slides on a linear track under current control (equivalent to closed-loop control of motor force), position control, and admittance control. We show proof-of-concept that novel velocity profiles of the robotic handle can differentially alter

gait parameters. The robotic emulator can therefore be used to identify and test controllers that could be implemented on and guide the design of mobile robotic walking aids in the future.

II. Device Design and Validation

A. Design criteria

By using a device that moves on a fixed track rather than a mobile robot, we use less of the device's power capabilities for self-locomotion and have more power for emulating physical interactions with the human. A prior study showed that humans prefer walking with a mobile humanoid robot with fewer degrees of freedom (i.e. very stiff arms and a compliant admittance-controlled base) [11], suggesting that a simple one-degree-of-freedom device is sufficient to examine principles of physical interaction in human-robot partnered walking.

To emulate human movement, the robot's bandwidth should be at least 6Hz for position control and up to 12Hz for force control based on previous studies examining gait kinematics [12] and human-human hand interactions [13]. Additionally, as human cutaneous mechanoreceptors can sense frequencies up to 1khz [17], robotic devices and controllers for human-robot interaction should avoid unintentional vibrations in this range.

B. Hardware

The hand-contact robotic device Slidey was developed to meet the design criteria above. A linear stage slides on a one-degree-of-freedom track powered by a linear induction motor; two handles are attached to the sensing face of a 6-axis force-torque sensor (model: 9105-T-GAMMA SI-32.2.5, ATI Industrial Automation, NC, USA), which is in turn fixed to the linear stage (Fig. 1). The linear stage has a 5.34 m stroke (model: 2XBLDM-B04, H2W Technologies, Inc., CA, USA) driven by a servo drive (Xenus XSJ-230-10, Copley Controls, MA, USA). The position of the linear stage is measured by a 1-um resolution linear encoder (LM10, Renishaw, Wotton-under-Edge, England). The motor has a 6.6 N/Amp motor constant and a 166.6 N force output at 10% duty cycle. The servo drive is configured in current control mode that supports 4.43 Amp continuous and 10 Amp peak current, resulting in approximately 55.2 N continuous force and 110 N peak force.

The user interface is designed to be ergonomic and versatile, allowing adjustability for different users and force and position information for different modes of use. The handles were custom-designed and 3D printed to mimic the shape and size of a doorknob. The location of each handle can be adjusted to accommodate the different distances between arms for each user. The handles can be mounted on either side of the device, allowing for forward walking in either direction, and one handle can be completed removed to test one-handed vs. bimanual hand interactions. The height of the handles can be adjusted to allow each user to maintain a comfortable arm posture of elbows bent at 90 degrees and wrists flat.

Multiple safety features are implemented via analog circuitry and digital controls. A "dead-man's" switch is embedded in one handle and depressed by the user's palm when holding the handle during normal operation. Letting go of the handle in shuts off power to the servo drive. Emergency stop buttons

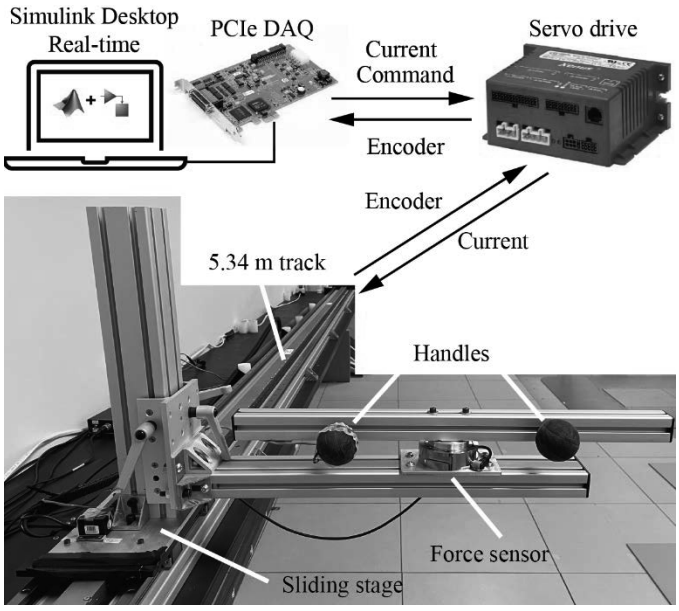

Fig. 1: Device components and communication pathways

connected directly to the servo drive power are positioned at the main control computer and at the far end of the track. A 10 Amp fuse is installed in series with the servo drive power. A velocity limit of 9 m/s is implemented in the servo drive software.

C. Control architecture

The computer controlling Slidey runs Simulink Desktop Real-Time (SDRT) software (Mathworks, MA, USA) that commands the servo drive, which runs its own lower-level current controller. SDRT runs at 1khz and outputs an analog voltage command via a 16-bit PCI DAQ board (PCIe6323, National Instruments, TX, USA) to the servo drive running at 15khz, which converts the voltage signal to a current command at a 1:1 ratio with 12-bit resolution. We chose to use current control instead of position control mode in the low-level controller as to avoid loss of position resolution over the long stroke of the linear motor. Given a track length of 5.34 m, 12-bit resolution of the servo drive would result in a position command resolution of 1.2 mm, which we deemed insufficient for emulating smooth hand motions during walking. The servo drive acquires linear encoder data at 20 MHz.

The force/torque sensor streams data at 7 khz over Ethernet (Net F/T) to SDRT. The sensor has a resolution of 1/160 N in the direction of walking. Interaction force and encoder position are recorded at 1 khz in SDRT.

Custom Simulink code was written to realize current, position, and admittance control. Current control is implemented via current commands from SDRT to the servo drive (Fig. 2a). Closed-loop position control is implemented by inputting an analog encoder signal to SDRT, calculating desired position, and outputting a current command to the servo drive (Fig. 2b). Admittance control is implemented by inputting both the analog encoder signal and the analog signal from the force sensor to SDRT, calculating desired position, and outputting a current command to the servo drive (Fig. 2c).

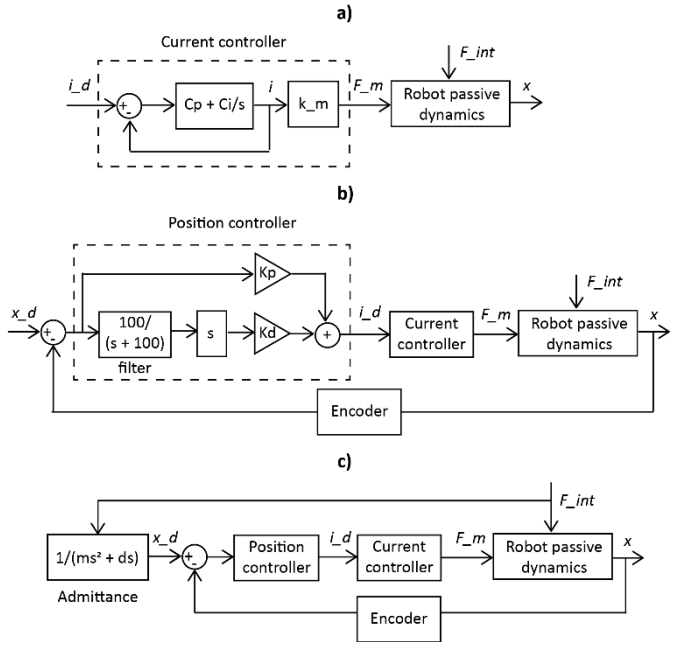

Fig. 3: Control diagrams for a) force control (i_d = desired current, i = actual current, Cp = proportional gain, Ci = integral gain, k_m = motor constant = 6.6 N/A, F_m = motor force, F_int = interaction force), b) position control, where Kp = proportional gain and Kd = derivative gain, x_d = desired position, x = actual position, and c) admittance control, where m = virtual mass and d = virtual damping.

D. Performance validation

1) Current control

The parameters for the current controller (Fig. 2a) on the servo drive were tuned using the auto-tuning function in CME 2 software (Copley Controls, MA, USA) to maximize smoothness of operation. The final tuning gains obtained were Cp = 61, Ci = 40. To characterize the frequency response with these gains, we input sinusoids with amplitude of 2 Amps and frequencies logarithmically scaled between 1-1024 Hz and calculated bandwidth from the resulting Bode plot (Fig. 3). The -3dB bandwidth achieved was between 512 and 1024 Hz.

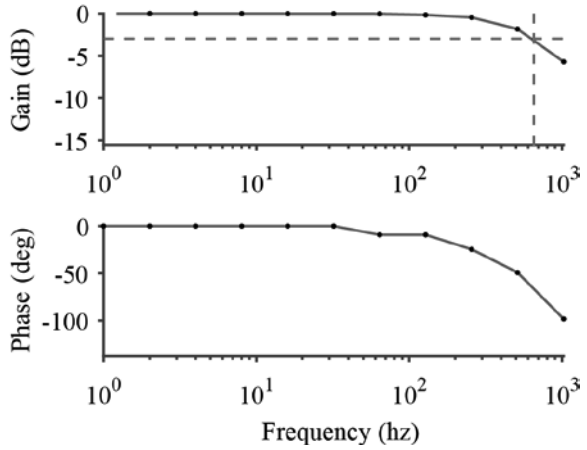

Fig. 2: Current controller Bode plot characterizing actual current input and desired current output. The dashed red line indicates the -3dB bandwidth.

2) Position control

Feedback gains for the closed-loop position controller (Fig. 2b) were manually tuned to result in smooth motion when commanding both a constant velocity and velocity pulses. The tuning gains used were Kp = 80 and Kd = 30. As position commands from the high-level controller are converted into current commands at the low-level controller, and we already calculated the bandwidth of the current controller, we next calculated the bandwidth of our system for desired position inputs and actual position outputs. We input sinusoids with velocity amplitude of 0.2 m/s and frequencies up to 20hz and calculated the 3dB bandwidth from the resulting Bode plot (Fig. 4). The bandwidth achieved was 5.84 Hz.

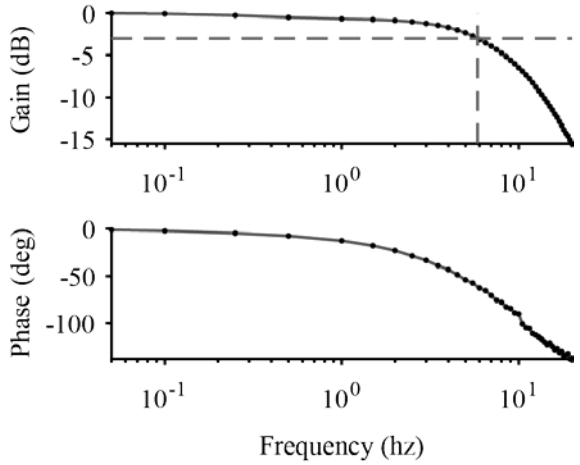

Fig. 4: Position controller Bode plot characterizing actual position output and desired position input. The dashed red line indicates the -3dB bandwidth.

3) Admittance control

We validated our admittance controller by measuring actual (x) and desired (x_d) position while a person held on to the handles of the device and a) walked at preferred velocity and b) stood in place and exerted sinusoidal forces at fixed frequencies. We chose admittance values of m = 5 N/(m/s^2) and b = 2.5 N/(m/s) based on anecdotal responses from the person about when they felt like the device did not affect their walking. Our human walking data showed a cross-correlation of 1.00 between actual and desired position with lag < 1ms (Fig. 5a). As the human could only move their arms/hands at a maximum frequency ~2hz, our Bode plot includes frequencies up to this limit. The results show that we have adequate bandwidth for admittance control in a realistic range of human hand/arm motions, i.e. we achieved a gain of -0.69 dB at 2hz (Fig. 5b).

III. Human User Testing

A. Velocity profiles to alter a specific gait parameter

As both force and admittance control have been previously demonstrated to alter human walking, we focus on demonstrating the effects of a novel velocity controller on gait parameters. Humans alter both step length and step frequency in equal proportions over a range of speeds during unaided walking [14], [15], so we sought to dissociate changes in these two gait parameters using Slidey.

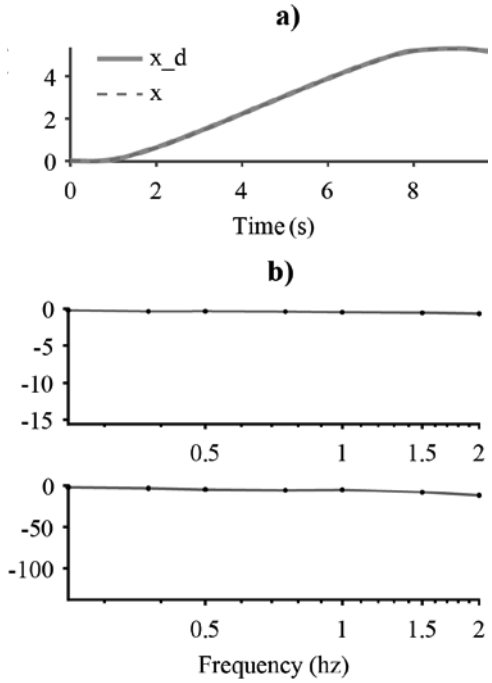

Fig. 4: Admittance control validation. a) Desired (x_d) and actual (x) robot position while a person held the handles of the device and walked at preferred speed under admittance control. b) Bode plot for desired and actual position during sinusoidal force inputs from human arm/hand motion.

We designed custom robot velocity profiles with velocity biases at different magnitudes and transient velocity pulses at different frequencies (Fig. 6a) implemented via position control. We hypothesized that the robot's velocity bias (b) at the hand would affect average human walking speed (vH) while the robot velocity pulse frequency (fR) would affect average human step frequency (fH) (Fig. 6a, b). Given the relationship that average walking speed is the product of average step length (L) and average step frequency (vH = L*fH), we varied the robot bias magnitude and pulse frequency to target changes in human gait speed, step frequency, and step length (Table 1).

The experiment had 3 conditions (Alter Gait Speed, Alter Step Frequency, and Alter Step Length) with 3 levels (below, at, and above preferred gait parameter value) per condition. 5 trials were performed for each level of each condition. Preferred values for each gait parameter were obtained from unaided overground walking.

Alter Gait Speed was the control condition, where velocity bias magnitudes (without pulses) were set to desired gait speed (b = vd). This condition established preferred step frequency and step length changes for comparison to the pulsed conditions.

We then aimed to independently alter either step frequency or step length as walking speed varied. During Alter Step Frequency, we set pulse frequency to desired step frequency (fR = fd) based on maintaining a constant preferred step length (Lp), i.e., vH = Lp * fd. During Alter Step Length, we maintained preferred step frequency (fR = fp) but adjusted the ratio between the bias speed and the step frequency (b/fR) to achieve a desired step length (Ld).

TABLE I. CONDITIONS, LEVELS, AND PARAMETER VALUES

Condition	Parameter		Level		
	Human	*Robot*	*Below*	*Preferred*	*Above*
Alter Gait Speed	vd	b	0.8*vp	vp	1.2*vp
Alter Step Frequency	fd	fR	0.8*fp	fp	1.2*fp
	v	b	0.8*vp	vp	1.2*vp
	L	b/fR	Lp	Lp	Lp
Alter Step Length	Ld	b/fR	0.7*Lp	Lp	1.5*Lp
	v	b	0.8*vp	vp	1.2*vp
	f	fR	1.2*fp	fp	0.8*fp

B. *Experiment setup*

A young adult (age 27 years, height 1.85 m, weight 106 kg) without neurological or physical impairments was recruited from Emory University (IRB00082414) to participate in user testing. Retroreflective markers were attached to the participant's body according to the Lower Body Plug-in-Gait model with an additional marker at the left shoulder and recorded at 120 hz with a 10-camera motion capture system (Vicon Nexus, Oxford, UK). Gait parameters of forward speed, step frequency, and step length were calculated from motion capture data of shoulder and heel markers (Fig. 6b, c).

Because we wish to develop a robot that is intuitive to use, the participant was not given explicit instructions on how to walk with the robot, other than to maintain a similar starting posture at the beginning of each trial and to step with the left foot first. The participant was only instructed to hold the robot handles "like doorknobs," maintain their arm posture (elbows bent at 90 degrees), stand with their weight mostly on one foot, and to "get ready to walk" after a series of auditory beeps at the beginning of each trial. To remove auditory and visual cues from the robot, the participant wore headphones playing white noise and was instructed to look straight ahead, not at the robot.

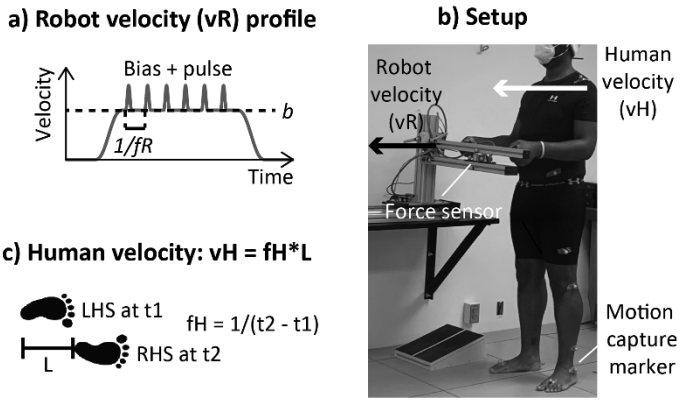

Fig. 6: a) Custom velocity profiles with velocity bias "b" and transient pulses at frequency "fR." were implemented in the robotic device to alter specific gait parameters. b) Participant kinematics were recorded via motion capture while they held the hand of the device and walked forwards. c) Human gait parameters of walking speed (vH), step frequency (fH), and step length (L) were calculated from motion capture data (LHS = left heelstrike, RHS = right heelstrike, t1 = time of LHS, t2 = time of RHS).

C. Data Analysis

We calculated gait parameters based on kinematics between the second and seventh heelstrike events of each trial, when gait approximated steady-state walking (from visual inspection of foot velocity) and excluded gait initiation and termination. All motion capture marker data was lowpass filtered at 30hz. Gait speed was calculated from the left shoulder marker's displacement over the steady state walking period. Step frequency was calculated from time between consecutive heelstrike events, averaged across all heelstrikes during the steady state walking period per trial. Step length was calculated as distance between heel markers at each heelstrike, averaged across all heelstrikes during the steady state walking period per trial. We normalized all gait parameters by preferred values obtained from walking without the robot.

To test if the participant dissociated step frequency and length, we compared regression slopes. We performed linear regression between gait parameter (speed, step frequency, step length) values and condition level (below, at, and above preferred). Then we tested if the slopes for the Alter Step Frequency and Alter Step Length conditions differed from the Alter Gait Speed control condition by examining the 95% CI's of regression coefficients for all conditions.

Finally, we examined relationships between hand interaction forces and foot velocity to understand how hand interactions affect walking. We obtained the anterior-posterior velocity for each foot from differentiating heel marker positions and then added the left and right velocities for combined foot velocity. We downsampled force data to match kinematic sampling frequency. After detrending and lowpass filtering both foot velocity and force data at 30hz, we performed cross-correlation on the two signals during the steady state walking period and obtained the time lag at maximum correlation.

D. Results

Kinematic results show that gait parameters changed in the intended directions (Fig. 7). Changing robot velocity bias (b) altered human gait speed below and above the preferred speed (Fig. 7a). Step frequency and step length increased in a coupled manner (i.e. at similar rates) as gait speed increases during the Alter Gait Speed condition. Gait speeds for the pulse conditions (Alter Step Frequency and Alter Step Length) were higher than the speeds for the control condition without pulses (Alter Gait Speed). In the Alter Step Frequency condition the robot pulse frequency at the hands increased step frequency (Fig. 7b, orange), while change in step length were attenuated (Fig. 7c, orange). Conversely, in the Alter Step Length condition, the changes in step frequency was attenuated (Fig. 7c, green) and step length was increased (Fig. 7c, green).

Slopes of regression lines mostly show intended dissociation between step frequency and step length in the pulse conditions. The slope was significantly greater for Alter Step Frequency than the other 2 conditions, suggesting that step frequency is most strongly affected in the condition designed to target step frequency (Fig. 7a). For step length, the slope of the Alter Step Length condition was not significantly different from that of the Alter Gait Speed condition, but the slope of the Alter Step Frequency condition was significantly less than the Alter Gait Speed condition (Fig, 7b). This suggests that the Alter Step Length condition did not alter step length as strongly as we desired, but the Alter Step Frequency condition resulted in more constant step length than the Alter Gait Speed control condition.

We observed transient peaks in anterior-posterior hand force that correlated in timing with AP foot velocity. We limited our analysis to the Alter Step Frequency condition because it was effective at altering gait parameters. Correlation between hand force and foot velocity was weakest when robot pulse frequency was at preferred step frequency (mean r = 0.14) and stronger when pulse frequency was below preferred step frequency (mean r = 0.36) or above preferred step frequency (mean r = 0.41). Hand force lagged foot motion slightly when hand pulse frequency was at preferred step frequency (mean lag = 0.04 s) Hand force lagged foot motion more when hand pulse frequency was below preferred step frequency (mean lag = 0.24 s). Hand force led foot motion when hand pulse frequency was above preferred step frequency (mean lag = -0.14 s).

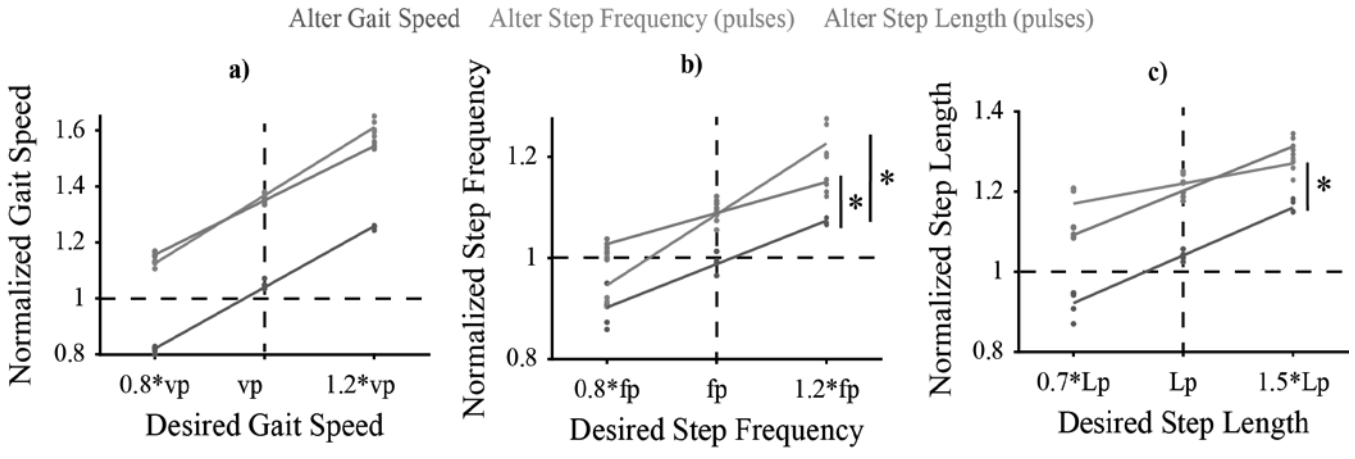

Fig. 7: Gait parameter results. Colors denote condition (i.e. gait parameter to be altered). Dots denote individual trial data and lines denote regression to trial data. Regression line slopes significantly different from that of the control condition (Alter Gait Speed) are denoted with an asterisk (*). a) Mean gait speed achieved vs. desired gait speed, b) mean step frequency vs. desired step frequency, and c) mean step length vs. desired step length.

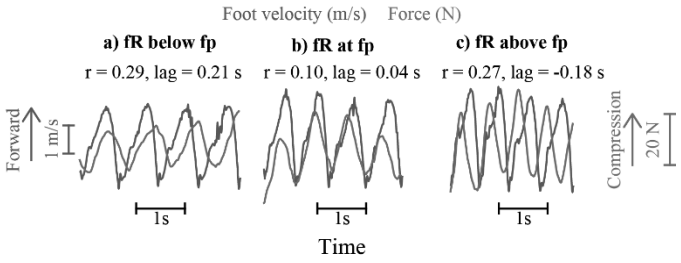

Fig. 8: Sample data of combined (left + right) foot velocity and hand interaction force with cross-correlation calculated during steady-state for each trial. As the data is detrended, larger relative values indicate greater forward velocity foot velocity and greater compressive force.

IV. Discussion

To our knowledge, this is the first pHRI robot capable of manipulating human hand interactions in a biologically-relevant way to alter not just how fast people walk, but also how they achieve that behavior. The device has more than sufficient capability to reliable emulate forces (>500 Hz) and motions (~6Hz) within the bandwidths observed in human walking and in human-human hand interactions. Thus, the device can be used to test a variety of pHRI and emulate pHHI paradigms.

As proof of concept, we demonstrate the ability of the device to preferentially alter step frequency or step length with gait speed, a result not previously demonstrated in hand-contact robotic walking aids. This effect was achieved without explicit instructions to the user, by changing the timing of transient velocity pulses to the hands during walking. The ability to systematically and intuitively alter gait parameters through hand forces provides promise for the use of hand-contact devices to improve walking quality, and not just speed.

Relationships between hand interaction forces and gait kinematics may further reveal the causality between hand interactions and walking. Our initial data show that forces at the hand are nearly time-synchronized with foot motions when the robot pulses at preferred step frequency. Hand forces lag foot motions when robot pulse frequency is below preferred step frequency, and lead foot motions when pulse frequency is above preferred. However, it is unclear whether the forces are due to the user anticipating or reacting to the hand motions. Further analysis may help elucidate mechanisms of how haptic information at the hands affects control of walking.

Our new robot Slidey can be used to implement, discover, and test a variety of different controllers. Specifically, it can be used to emulate strategies of pHHI not previously explored in pHRI and explore novel controllers to target specific changes in gait parameters. Developing a high-fidelity robotic emulator may be a critical step to better understand principles of pHRI and to provide design specification for mobile robotic walking aids to target different gait deficits.

Acknowledgment

The authors wish to thank the Neuromechanics Lab. This work was funded by the National Science Foundation Division of Civil, Mechanical, and Manufacturing Innovation M3X–Mind, Machine, and Motor Program: NSF CMMI 1762211 and NSF CMMI 1761679.

References

[1] A. Z. Zivotofsky and J. M. Hausdorff, "The sensory feedback mechanisms enabling couples to walk synchronously: An initial investigation," *Journal of NeuroEngineering and Rehabilitation*, vol. 4, no. 1, p. 28, Aug. 2007, doi: 10.1186/1743-0003-4-28.

[2] F. Sylos-Labini, A. d'Avella, F. Lacquaniti, and Y. Ivanenko, "Human-Human Interaction Forces and Interlimb Coordination During Side-by-Side Walking With Hand Contact," *Front. Physiol.*, vol. 9, p. 179, Mar. 2018, doi: 10.3389/fphys.2018.00179.

[3] A. Sawers, T. Bhattacharjee, J. L. McKay, M. E. Hackney, C. C. Kemp, and L. H. Ting, "Small forces that differ with prior motor experience can communicate movement goals during human-human physical interaction," *J NeuroEngineering Rehabil*, vol. 14, no. 1, p. 8, Jan. 2017, doi: 10.1186/s12984-017-0217-2.

[4] M. Wu, L. Drnach, S. M. Bong, Y. S. Song, and L. H. Ting, "Human-Human Hand Interactions Aid Balance During Walking by Haptic Communication," *Frontiers in Robotics and AI*, vol. 8, p. 357, 2021, doi: 10.3389/frobt.2021.735575.

[5] G. U. Sorrento, P. S. Archambault, J. Fung, and C. Feil-Oberfeld, "The effects of haptic forces on locomotion and posture in post-stroke and elderly adults," in *2015 International Conference on Virtual Rehabilitation (ICVR)*, Jun. 2015, pp. 147–148. doi: 10.1109/ICVR.2015.7358622.

[6] G. U. Sorrento, P. S. Archambault, and J. Fung, "Adaptation and post-adaptation effects of haptic forces on locomotion in healthy young adults," *Journal of NeuroEngineering and Rehabilitation*, vol. 15, no. 1, p. 20, Mar. 2018, doi: 10.1186/s12984-018-0364-0.

[7] D. M. Stramel, R. M. Carrera, S. A. Rahok, J. Stein, and S. K. Agrawal, "Effects of a Person-Following Light-Touch Device During Overground Walking With Visual Perturbations in a Virtual Reality Environment," *IEEE Robotics and Automation Letters*, vol. 4, no. 4, pp. 4139–4146, Oct. 2019, doi: 10.1109/LRA.2019.2931267.

[8] H. Lee *et al.*, "Development of a Robotic Companion to Provide Haptic Force Interaction for Overground Gait Rehabilitation," *IEEE Access*, vol. 8, pp. 34888–34899, 2020, doi: 10.1109/ACCESS.2020.2973672.

[9] M. Alwan, A. Ledoux, G. Wasson, P. Sheth, and C. Huang, "Basic walker-assisted gait characteristics derived from forces and moments exerted on the walker's handles: Results on normal subjects," *Medical Engineering & Physics*, vol. 29, no. 3, pp. 380–389, Apr. 2007, doi: 10.1016/j.medengphy.2006.06.001.

[10] A. Abellanas, A. Frizera, R. Ceres, and J. A. Gallego, "Estimation of gait parameters by measuring upper limb–walker interaction forces," *Sensors and Actuators A: Physical*, vol. 162, no. 2, pp. 276–283, Aug. 2010, doi: 10.1016/j.sna.2010.05.020.

[11] T. L. Chen *et al.*, "Evaluation by Expert Dancers of a Robot That Performs Partnered Stepping via Haptic Interaction," *PLoS ONE*, vol. 10, no. 5, p. e0125179, 2015, doi: 10.1371/journal.pone.0125179.

[12] R. Khusainov, D. Azzi, I. E. Achumba, and S. D. Bersch, "Real-Time Human Ambulation, Activity, and Physiological Monitoring: Taxonomy of Issues, Techniques, Applications, Challenges and Limitations," *Sensors (Basel, Switzerland)*, vol. 13, no. 10, p. 12852, Oct. 2013, doi: 10.3390/s131012852.

[13] K. B. Reed, M. Peshkin, M. J. Hartmann, J. E. Colgate, and J. Patton, "Kinesthetic interaction," in *9th International Conference on Rehabilitation Robotics, 2005. ICORR 2005.*, Jun. 2005, pp. 569–574. doi: 10.1109/ICORR.2005.1502027.

[14] N. Sekiya, H. Nagasaki, H. Ito, and T. Furuna, "The invariant relationship between step length and step rate during free walking," *Journal of Human Movement Studies*, vol. 30, no. 6, pp. 241–257, 1996.

[15] B. Bogen, R. Moe-Nilssen, A. H. Ranhoff, and M. K. Aaslund, "The walk ratio: Investigation of invariance across walking conditions and gender in community-dwelling older people," *Gait & Posture*, vol. 61, pp. 479–482, Mar. 2018, doi: 10.1016/j.gaitpost.2018.02.019.

[16] M. S. Bryant, A. Pourmoghaddam, and A. Thrasher, "Gait changes with walking devices in persons with Parkinson's disease," *Disability and Rehabilitation: Assistive Technology*, vol. 7, no. 2, pp. 149–152, Mar. 2012, doi: 10.3109/17483107.2011.602461.

[17] S. Mack, E. R. Kandel, T. M. Jessell, J. H. Schwartz, S. A. Siegelbaum, and A. J. Hudspeth, *Principles of Neural Science, Fifth Edition*. McGraw Hill Professional, 2013.